Critical Dependence of Polarization Phenomena on Conductivity in Ferroelectric Polymers

S.N. Fedosov[1,*], H. von Seggern[2,†]

[1] *Department of Physics and Materials Science, Odessa National Academy of Food Technologies, 112, Kanatnaya Str., 65039 Odessa, Ukraine*

[2] *Institute of Materials Science, Darmstadt University of Technology, 23, Petersenstrasse, 64287 Darmstadt, Germany*

Experimentally obtained data on the polarization dynamics in polyvinylidene fluoride, a typical ferroelectric polymer, are analyzed during initial poling, short circuiting and polarization switching. Considering a two-component structure of the samples, namely, presence of ferroelectric and non-ferroelectric phases, it is shown that value and stability of the ferroelectric polarization significantly depend on conductivity and space charges. Application of a simple two-layer theoretical model with an explicit conductivity allowed explaining such important features, as slow development and switching of the ferroelectric polarization and a partial back-switching of the already formed polarization after short-circuiting of the sample.

Key words: Polarization, Conductivity, Space charge, PVDF, Ferroelectric polymers.

PACS numbers: 77.84. – s, 77.84.Jd, 73.61.Ph

1. INTRODUCTION

Ferroelectric polymers like polyvinylidene fluoride (PVDF) and its copolymers have attracted attention during the last years due to a promising combination of high residual polarization and good mechanical properties [1].

After discovering strong piezoelectricity [2], pyroelectricity [3] and ferroelectricity [4] in PVDF the polymer became an object of numerous studies directed to basic understanding and technical applications. Many articles have been published on various properties of PVDF and its copolymers comprising structural, morphological, and electrical data. Although initially expected wide-scale application of PVDF has not been realized until now, it still remains a typical representative of a ferroelectric polymer family. Comprehensive review papers have been published by Lovinger [5], Gerhard-Multhaupt [6], Furukawa [7,8], Kepler and Anderson [9], Sessler [10], Kepler [11], Eberle et al [12], and Broadhurst and Davis [13].

Most controversially discussed is the role of charge in the polarization process of PVDF and other ferroelectric polymers. Originally PVDF was considered as a strongly dipolar electret material with a thermally frozen-in polarization where high-temperature-and-low-electric-field poling was utilized.

Only after the discovery [14] that PVDF is a ferroelectric material with a spontaneous polarization, high DC fields were employed to align and switch the polarization without thermal activation. Subsequently, thermoelectret poling [15-18] was gradually replaced by high-field-room-temperature poling [19-26] without thermal freezing of the induced polarization. At that time there was no room for space charge in the model of polarization build-up and switching, because the switching time in PVDF and its copolymers was considered to be of the order of microseconds at high fields [4, 7, 8]. Therefore, conductivity and space charge were considered as secondary and even interfering side effects.

Interest to the charge in PVDF was aroused again when Eisenmenger et al. put forward a qualitative charge trapping model assuming that dipoles in PVDF are intrinsically unstable and their preferential orientation can be fixed only by charges trapped at the dipole or domain surfaces [27]. However, their assumption of instantaneous switching of dipoles and their back-switching, if not stabilized by charges [27-29], has not been proved experimentally, since the resulting large displacement currents during back-switching have not been ever observed.

The first introduction of charge into the model was made by Furukawa et al. [30] for PZT-polymer composites. In these composites the presence of a non-ferroelectric component along with a ferroelectric one delays the polarization switching due to the effect of conductivity in both components. For a long time this idea has not been adopted to ferroelectric polymers and other two-phase systems exhibiting clearly a similar structure of ferroelectric and non ferroelectric phases. Only in recent studies the importance of conductivity and screening charge formation has been pointed out in PVDF [21-26] and its importance for polarization dynamics during initial poling, short-circuiting and polarization switching was demonstrated. It has been shown that the build-up of polarization in PVDF exhibits two stages with the second slow one controlled by the build-up of screening charges through intrinsic conductivity. This allowed one to explain a huge discrepancy between expected and observed poling and switching times in PVDF. Thus, it has been proved that in semicrystalline ferroelectric polymers like PVDF, compensating charges localized on the surface of crystallites are very important for obtaining a high and stable polarization.

There is especially one feature of the ferroelectric polymers and other ferroelectric materials, such as ceramics and ceramics-polymer composites, that was not given enough consideration so far. All these materials are basically two-phase systems with considerably different dielectric constants and polarization-field depend-

---

*[*] fedosov@optima.com.ua

[†] seggern@e-mat.tu-darmstadt.de

ences of the individual phases. For example, PVDF is a semicrystalline material with the amorphous phase occupying about 50 % of the polymer volume. It is clear that the amorphous part itself does not contribute to the residual polarization; nevertheless, it plays an important role in the temporal development of the ferroelectric polarization build-up in the ferroelectric crystallites.

During polarization build-up in ferroelectrics, the bound surface charge of the polarization generates a depolarization field that tends to switch back the electric field induced polarization to its initial state of a random distribution as soon as the electric field is removed by short-circuiting the sample [31, 32]. For preserving the obtained polarization under applied voltage, the depolarization field must at least partially be neutralized or compensated [27]. In the case of a mono-domain ferroelectric with deposited electrodes the compensation is done instantaneously by electrode charges. During short-circuiting subsequent to poling such additional compensation charge will remain in the electrodes thereby preventing undesirable depolarization.

Polarization phenomena in two-component ferroelectrics differ considerably from that of mono-domain materials. In this case, the depolarization fields existing in the ferroelectric crystallites cannot be compensated immediately due to the relatively small conductivity of this class of materials. Charge needs time to accumulate at the boundaries between ferroelectric and non-ferroelectric phases. Thus, a finite conductivity and therewith a finite time are needed to build up a complete local compensation of the ferroelectric depolarization fields [22, 24]. This time is known as Maxwell relaxation time of the individual materials.

In this paper all three important processes in two-component ferroelectric polymers are analyzed comprising initial poling, short circuiting and polarization switching. It is shown that a simple two-layer modeling can explain the behavior of polarization and its interrelation with conductivity and space charges.

2. EXPERIMENTAL

Experiments were carried out on 12.5 µm-thick bi-axially stretched PVDF samples from Kureha Co. with metal electrodes of 0.2 cm² area deposited either by vacuum evaporation or cathode sputtering. The crystallographic structure of the polymer under study exhibited almost equal portions of crystalline and amorphous phases. IR spectra taken by means of a Perkin-Elmer 1750 FTIR spectrometer indicated that the fraction of the ferroelectric β-phase in relation to the non-polar α-phase corresponded to a ratio of 70 : 30. The IR measurements on poled samples had shown that the interrelation between α and β phases remained unchanged after poling and switching.

Poling and switching experiments were performed utilizing an electrical circuit described elsewhere [21] and shown in Figure 1. The DC voltage U_0 was supplied by a conventional high voltage source buffered by a 0.5 µF high-voltage capacitor C large enough to support the required poling currents. Actual high voltage poling and polarization switching was performed by means of an electronic high voltage / high current push-pull switch from Behlke Co., Germany. It was possible to apply voltage pulses from 100 ns to 1000 s duration controlled by a re-

mote low-voltage pulse generator. Thereby, the voltage across the sample was switched from initially ground to high voltage and back to ground. This allowed one to stop the charging or switching polarization process within the time constant of the electrical circuit of about 50 ns. The measuring branch consisted of the sample having an apparent capacitance of about $C_s = 160$ pF at 100 V, a current limiting resistor $R_s = 500$ Ω and a series measuring capacitor $C_m = 0.2$ µF.
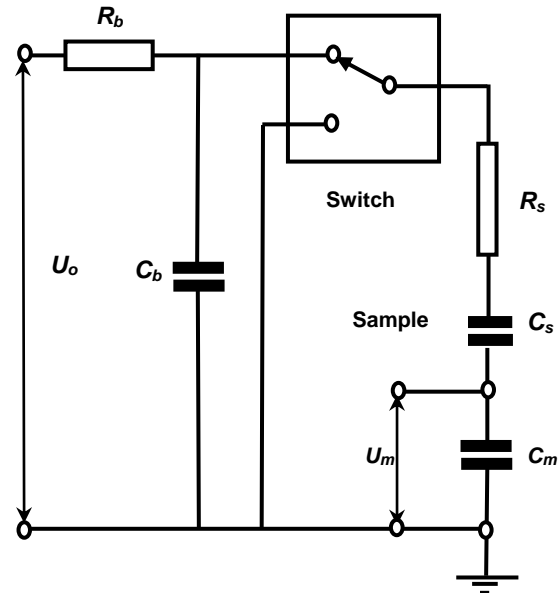

Fig. 1 – Schematic diagram of the experimental setup for poling of PVDF and switching of polarization

The voltage drop at the capacitor C_m was registered by means of a digital oscilloscope Tektronix TDS 510A connected through a high impedance operational amplifier ($R_{in} = 10^{13}$ Ω). Leakage of charges from the probe capacitor C_m due to parasitic currents to ground were tested and found to be negligible for the utilized measuring times.

The voltage at the series capacitor C_m was used to calculate the charge flowing through the sample during initial poling, short circuiting and polarization switching. The total "apparent" displacement D_1 included not only ferroelectric polarization current, but also a reversible capacitive current and the leakage one. Virgin samples were poled at $U_0 = 2$ kV, while the development of the total displacement D_1 was recorded. Subsequently each sample was fully polarized at 2.4 kV for 200 s followed by forward poling at $U_o = 2$ kV in the same direction in order to obtain D_2 curves containing all components of D_1, but the remanent polarization. Therefore, the ferroelectric polarization was calculated from a difference between D_1 and D_2. More details on processing experimental D_1 and D_2 curves can be found in [21].

The samples for the switching experiments were pre-poled by application of a voltage of 2.4 kV for 200 s and subsequent short-circuiting for 15 min. For switching, a DC voltage pulse of 2 kV was applied in the direction opposite to that of initial poling with pulse length from 10^{-6} to 100 s. After each switching experiment samples were reconditioned by application of 2.4 kV for 200 s in the pre-poling direction. The procedure to measure the back-switched polarization is described in the corresponding section.

3. INITIAL POLING

A phenomenological model of a two-phase system composed of ferroelectric and non-ferroelectric regions has been proposed. Taking into account the brick-like structure of isolated ferroelectric crystallites in PVDF [33], the real material is described by n alternating non-ferroelectric layers of the thickness d_1 each with a linear dielectric constant ε_1 and n ferroelectric layers of thickness d_2 with a linear dielectric constant ε_2 and a ferroelectric polarization P. It can be shown that the problem can generally be reduced to a two-layer system, as shown in Figure 2. Since the thickness of the sample is much smaller than the diameter of the samples, a one-dimensional model description can be considered.
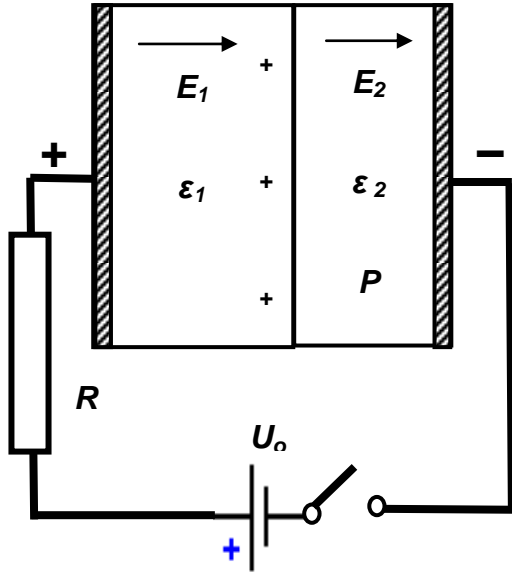
Fig. 2 – Geometry and principle of the setup.

Suppose a virgin sample is subjected to an instantaneously applied DC voltage U_0 through a current limiting resistor R_s. Then the electric fields E_1 and E_2 will appear in the non-ferroelectric and ferroelectric layers, correspondingly. In the ferroelectric phase the time and field dependent ferroelectric polarization P also exists. Assuming that there is a finite conductivity g, the total current density j is the same in the resistor, in the non-ferroelectric and ferroelectric regions and can be written as

$$j = \frac{U_0 - n(d_1 E_1 + d_2 E_2)}{AR_s} = \varepsilon_0 \varepsilon_1 \frac{dE_1}{dt} + gE_1 =$$
$$= \varepsilon_0 \varepsilon_2 \frac{dE_2}{dt} + gE_2 + \frac{dP}{dt} \qquad (1)$$

It can be recognized from equation (1) that there are capacitive and conductive currents in the non-ferroelectric phase, while a polarization current dP/dt is added in the ferroelectric phase. Since $E_1 \neq E_2$, a surface charge $\sigma(t)$ will accumulate at the phase boundaries with a rate determined by the charge balance equation

$$\frac{d\sigma}{dt} = g(E_1 - E_2). \qquad (2)$$

The field dependence of the quasi-stationary polarization $P_s(E_2)$ is assumed to be a non-linear function of E_2 in accordance with experimentally obtained results on hysteresis phenomenon in PVDF. $P_s(E_2)$ is simplified by the following function

$$P_s(E_2) = \begin{cases} 0 & E_2 < E_c \\ \dfrac{E_2 - E_c}{E_{sat} - E_c} \cdot P_{sat}; & E_c \leq E_2 \leq E_{sat} \\ P_{sat} & E_2 > E_{sat} \end{cases}, \qquad (3)$$

where P_{sat} is the maximum saturated polarization. $P_s(E_2)$ increases thereby linearly from zero up to P_{sat} for $E_c \leq E_2 \leq E_{sat}$ and saturates at $P = P_{sat}$ for $E_2 > E_{sat}$. Similar field dependence has been used before in model calculations of polarization build-up in ferroelectric polymers [34].

The dynamics of the ferroelectric polarization is described by a Debye-like relaxation equation used in many theoretical treatments of PVDF systems [34, 35]

$$\frac{dP}{dt} = \frac{P_s(E_2) - P}{\tau(E_2)}, \qquad (4)$$

where $\tau(E_2)$ is the field dependent switching time that can be expressed as [7]

$$\tau(E_2) = \tau_0 \exp\left(\frac{E_A}{E_2}\right), \qquad (5)$$

where τ_0 and E_A are material constants.

Expressions (1) to (5) form a set of non-linear differential equations solved numerically under initial conditions of $P(0) = 0$, $\sigma(0) = 0$ and results for E_1, E_2, P and σ are displayed in Figs. 3 and 4. All parameters used in the model calculation were carefully selected in accordance with published data [7, 11] or with experimental results [21]. Values of the parameters used in the model calculations are summarized in Table 1. Justifications for the selected values of the dielectric constants ε_1 and ε_2, conductivity g, the saturated polarization P_s, the coercive field strength E_c and the characteristic field E_s are given in [21]. Coercive field strength of 50 MV/m was found to be adequate to describe the observed experimental results, however, no severe attempt was made to optimize this value. Since the characteristic time constants of polarization growth for initial poling are not known, we adopted values of polarization switching in PVDF [7] with $\tau_0 = 20$ ns and $E_A = 1.2$ GV/m in equation (5). The conductivity value of $g = 3 \cdot 10^{-11}$ S/m was obtained experimentally within this study. Results of model calculations show principal agreement between experimentally measured and calculated values of polarization, as seen from Figure 3.

Table 1 – Values of parameters used in the model calculations of poling

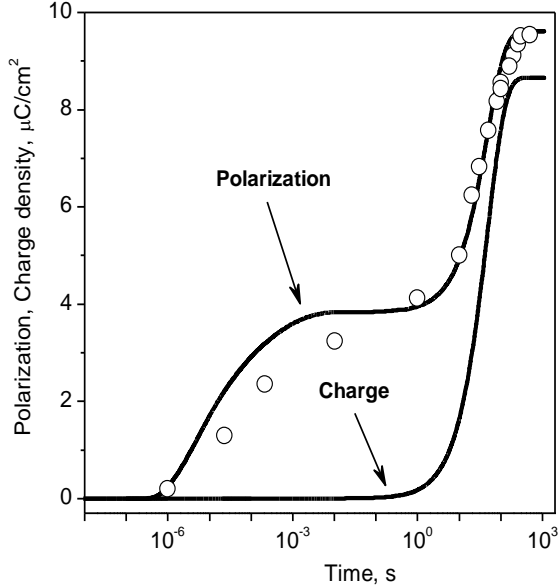| U_0	n	d_1	d_2	ε_1	ε_2	d
2 kV	42	200 nm	100 nm	19.6	12.9	12.5 µm
RC	g	P_r	E_s	E_c	τ_0	E_A
80 ns	$3 \cdot 10^{-11}$ S/m	13.1 C/cm²	200 MV/m	50 MV/m	20 ns	1.2 GV/m

Fig. 3 – Comparison of calculated values of polarization *P* with experimentally obtained ferroelectric polarization (open dots). The compensation charge is also plotted
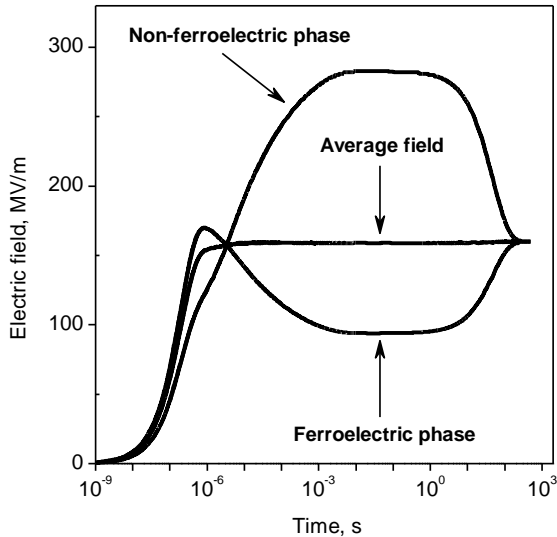

Fig. 4 – Calculated electrical field strength with time. $V_0 = 2$ kV, the Maxwell relaxation time is 15 s

The theoretical results show that during fast poling the ferroelectric polarization *P* in the ferroelectric phase grows at the expense of the electric field E_2. This leads to a fast decay of the electric field E_2 in the ferroelectric phase down to a value where polarization buildup stops due to too long poling times, as can be seen from equation (5) and Figure 4. Without conductivity, polarization built-up would slow down at about 10^{-4} s, and no further increase in polarization would be observed. In the presence of conductivity, however, polarization continues to grow, as can be seen from Figure 3. This is due to interfacial charge density *σ* that accumulates at the boundaries of the layers due to the finite conductivity and the different fields in the two layers, as seen from equation (2). It can be easily shown that the corresponding time constant can be described as the Maxwell relaxation time. The model calculation

shows impressively that this charge accumulation results in an increase of the electric field E_2 in the ferroelectric phase by screening the ferroelectric polarization *P*. The resulting currents are very small and often misinterpreted as pure conduction or leakage currents.

4. SHORT-CIRCUITING AND BACK-SWITCHING

Samples are short-circuited after poling. The ferroelectric polarization developed during poling is stable, if the depolarization field is properly neutralized or compensated. If this condition is not satisfied, a part of the already developed ferroelectric polarization P_F can switch back due to a change in the electric field which in some cases exceeds the breakdown strength during short circuiting. To distinguish experimentally between the back-switched part of the ferroelectric polarization P_{bs} and a reversible capacitive component of the total polarization P_L, we suggest the following procedure.

Suppose a sample is poled for a period of time t_1 and then short circuited for the time $\Delta t = t_2 - t_1$. Experimentally measured displacements $D_1(t_1)$ and $D_1(t_2)$ can be presented as

$$D_1(t_1) = P_L + P_F + D_{cond} \qquad (6)$$

$$D_1(t_2) = D_{cond} + P_F - P_{bs} \qquad (7)$$

where D_{cond} is the conductivity contribution to the total measured displacement and P_L is the reversible part of the polarization, e.g., due the purely capacitive part of the sample.

Note that D_{cond} remains unchanged resulting from the fact that the average field after short-circuiting is zero and therefore charges accumulated due to conduction during poling cannot leave the sample anymore.

Then two additional experiments are performed. The sample is poled to saturation for very long time using the same voltage polarity, but larger voltage amplitude. Now it can be assumed that the sample contains already the stable ferroelectric polarization P_{sat}. If a forward poling is now performed on this fully polarized sample, the displacement $D_2(t_1)$ at the end of poling contains only the reversible component P_L and the non reversible conduction term D_{cond}

$$D_2(t_1) = P_L + D_{cond} \qquad (8)$$

The sample is then short circuited and P_L disappears, so that $D_2(t_2)$ can be described as

$$D_2(t_2) = D_{cond} \qquad (9)$$

The back-switched part P_{bs} of the ferroelectric polarization can then be deduced from equations (6) to (9) by processing the experimental curves $D_1(t)$ and $D_2(t)$

$$P_{bs} = \left[D_1(t_1) - D_1(t_2) \right] - \left[D_2(t_1) - D_2(t_2) \right] \qquad (10)$$

For obtaining the dynamics of back-switching for a fixed poling time, one can subtract the whole curve $D_2(t)$ from $D_1(t)$ starting from the moment t_1 of short circuiting.

For two poling times t_1 of 200 s and 10 ms the complete dynamics of initial poling and the back-switching have been measured, whereby the total short circuiting time was 200 s. The resulting experimental curves are

plotted in Figs. 4 and 5. The temporal buildups of the experimentally measured ferroelectric polarization exhibit fast and slow components of the polarization buildup in the case of the long poling times. No back switching is observed during subsequent short-circuiting for a ferroelectric polarization of 9.45 µC/cm², which is the maximum achievable value at the applied field of 160 MV/m. During the poling time of 10 ms the ferroelectric polarization of only 2.5 µC/cm² was developed decaying considerably during short-circuiting, as seen from Figure 6. A fraction of about 1.2 µC/cm² has switched back.

In order to understand the temporal development of the back-switching, the electric field strengths E_1 in the non-ferroelectric component and E_2 in the ferroelectric component, as well as the ferroelectric polarization P_F and the interfacial charge σ during the short circuiting have to be analyzed. This was done utilizing the same model as for the description of initial poling.

The polarization $P_F(t)$ stays constant at $P_F(t) = P_{sat}(E_2)$ until the absolute value of E_2 is smaller than that of the coercive field E_c. It is assumed to decrease linearly when E_2 exceeds E_c, following the equation

$$P_s(E_2) = P_F(t=0) - \frac{2P_{sat}\left(E_2 - E_c\right)}{E_s - E_c} \qquad (11)$$

It is assumed that the voltage U_0 applied to the sample, as well as the average field strength during short-circuiting decays exponentially to zero with a characteristic time constant of about $\tau = 80$ ns determined by the sample capacitance $C_s = 160$ pF and the current limiting resistor $R_b = 500$ Ω. It yields

$$U(t) = n\left(d_1 E_1 + d_2 E_2\right) = U_0 \exp\left(-\frac{t}{\tau}\right) \qquad (12)$$

From continuity of the displacement vector at the boundaries between non-ferroelectric and ferroelectric layers it follows that

$$\varepsilon_o \varepsilon_1 E_1(t) = \varepsilon_o \varepsilon_2 E_2(t) + P_F(t) - \sigma(t) \qquad (13)$$
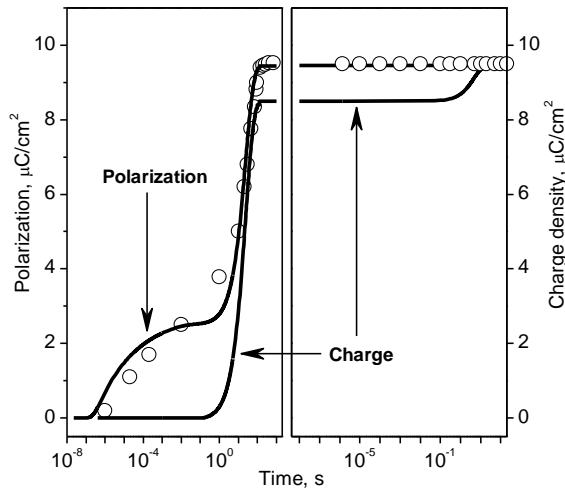

Fig. 5 – Experimental and calculated dynamics of the ferroelectric polarization in PVDF and calculated evolution of the interfacial charge (right scale) during initial poling at 2 kV for 200 s (left figure) and subsequent short circuiting (right figure). Short circuiting occurs at $t = 200$ s (left figure) and $t = 0$ (right figure)

It is clear from equations (12) and (13) that the field E_2 in the ferroelectric region changes its sign from positive to negative during the short-circuiting. However, the polarization P_F, due to its ferroelectric nature, remains constant $P_F(t) = P_{F0}$ as long as the absolute value of the electric field E_2 remains smaller than that of the coercive field E_c. If E_2 surpasses E_c, back-switching of a part of the polarization P_F occurs with the value of E_2 decreasing again, as can be seen from equation (13). The process of the back-switching will go on until E_2 reaches E_c. The dynamics of the back-switching is governed by the generally accepted field dependent relaxation time [4] in combination with a differential equation of the Debye type [22-24]

$$\frac{dP_F}{dt} = \frac{P_{sat}(E_2) - P_F}{\tau_0 \exp\left(\dfrac{E_A}{|E_2|}\right)} \qquad (14)$$

where τ_0 is the characteristic switching time constant and E_A the activation field as used before.

Expressions (11) to (14) form a set of differential equations sufficient to calculate the temporal development of E_1, E_2, P_F and σ during short-circuiting following initial poling.

The $P_F(t)$ function is of particular importance, since it determines the stability of the ferroelectric polarization and the value of back switching. The set of equations was solved numerically for three different initial conditions shown in Table 2 representing the three different cases of back-switching: after a long poling of 200 s, intermediate poling of 10 ms and short poling of 1.4 µs.

Initial values of the electric fields $E_1(0)$ and $E_2(0)$, the ferroelectric polarization $P_F(0)$ and the interfacial charge $\sigma(0)$ were calculated from the model described in the initial poling section. Results of model calculations of initial poling for 200 s and 10 ms and the corresponding short-circuiting processes are presented in Figs. 6 and 7 and discussed below.

As one can see from Figs. 4 and 6, for long poling times of 200 s the depolarization field is effectively screened by the accumulated interfacial charge σ at the end of poling. In this case, the electric fields in the ferroelectric and non-ferroelectric regions are equal to the average field prior to short-circuiting. After short-circuiting, the field in the ferroelectric component (Figure 7), though being negative, remains smaller than

Table 2 – Initial conditions for short circuiting

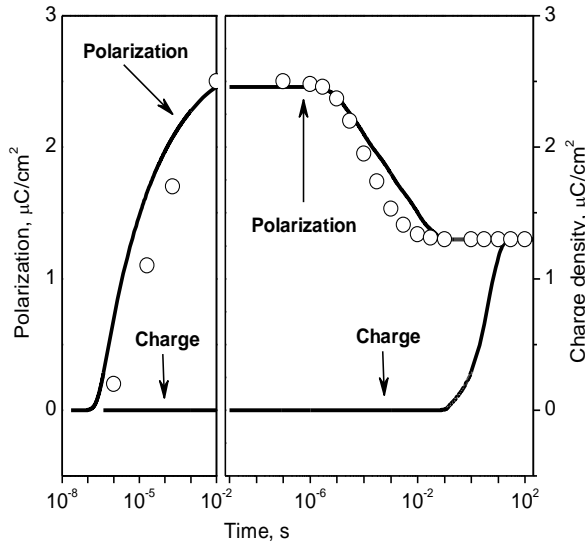| Description	Symbol	Unit	Case 1	Case 2	Case 3
Poling time	t_1	s	$1.4 \cdot 10^{-6}$	10^{-2}	200
Field in the non-ferroelectric part	$E_1(0)$	MV/m	156	197	160
Field in the ferroelectric part	$E_2(0)$	MV/m	162	81	160
Average field	$E_{av}(0)$	MV/m	160	160	160
Ferroelectric polarization	$P_F(0)$	µC/cm²	0.86	2.46	9.45
Interfacial charge	$\sigma(0)$	µC/cm²	0	0	8.5

Fig. 6 – Experimental and calculated dynamics of the ferroelectric polarization in PVDF and calculated evolution of the interfacial charge (right scale) during initial poling at 2 kV for 10 ms (left figure) and subsequent short circuiting (right figure). Short circuiting occurs at $t = 10$ ms (left figure) and $t = 0$ (right figure)

the coercive field and therefore the back switching of polarization will not occur. The resulting electric fields finally become zero due to conduction. The compensating charges, which results from the differences in the dielectric constants under applied voltage, now gradually disappear and only the compensation charges of the ferroelectric polarization remain.

For poling times of 10 ms the temporal development of the electric fields in short circuit is considerably different from that for the long poling times (see Figs. 5 and 7). The initial value of the electric field in the ferroelectric part is rather low compared to that in the
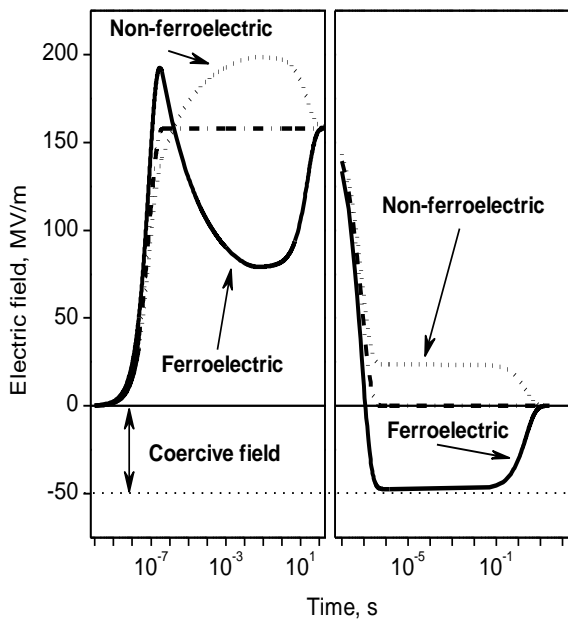

Fig. 7 – Calculated development of the field strength in the ferroelectric (solid line) and nonferroelectric (dotted line) components of PVDF during initial poling at 2 kV for 200 s (left figure) and subsequent short circuiting (right figure). The average field is shown by a dash-dotted line

non-ferroelectric region. Equation (13) explains why the differences between the electric fields E_1 and E_2 are so large at the end of poling in comparison to the results of Figure 7. The reason is that the field E_2 in the ferroelectric part decreases considerably at the expense of the formed polarization P_F meaning that the electric field E_1 increases correspondingly. Since the ferroelectric polarization is not compensated by interfacial charges, the fields E_1 and E_2 differ considerably at the end of poling. During short circuiting the average field drops to zero in about 1 μs, while E_2 decreases during this time to values of about -125 MV/m, thereby exceeding the coercive field of -50 MV/m considerably; so back switching is initiated. For fields ranging from -125 MV/m to -50 MV/m the switching time constant varies from 0.3 ms to 530 s. From equation (13) it is apparent that an increase of σ is equivalent to a decrease of P_F. The resulting effect on the electric field E_2 in the ferroelectric part is the same: as soon as the field becomes smaller than the coercive field, back switching stops.

In Figure 6 the dynamics of the calculated ferroelectric polarization and the compensating charges are displayed for the 10 ms poled sample. It can be seen that the switched back polarization amounts to 1.16 μC/cm², i.e. almost half of the polarization developed during initial poling. The back switching occurs in the short time period of short-circuiting between 10 μs and 0.1 s. As one can also see from Figure 6, this time is not long enough to allow the compensating charges to rearrange. The complete screening with zero field everywhere and equality between polarization and charge is achieved after about 50 s which corresponds to the well-known Maxwell relaxation time [1]. One can see from Figure 6 that there is general agreement between experimentally measured and calculated polarization.

In the case of model calculations for very short poling time of $t_1 = 1.4$ μs (not shown here) similar electric field buildups and decays are observed as for the long term poled sample (see Figure 7). No back switching is expected in this case, since the electric field in the ferroelectric part does not exceed the coercive field E_c during the short-circuiting process. Unfortunately, we were unable to verify experimentally whether there is back switching in this case, because the actual ferroelectric component is too small and due to signal-to-noise ratio problems the back switched part is not uniquely recognizable.

Concerning the interpretation of the experimental data with the applied model, conductivity and charges are needed at the interfaces to avoid back switching. The model proposes that the charges at the boundaries of the crystallites or domains reduce the depolarization field, which is the only reason for back switching. Therefore back switching is only possible, if the depolarizing field in the ferroelectric phase during short-circuiting exceeds the coercive field E_c. Such a behavior can be seen from Figure 8.

In this case the sample is poled for 10 ms and about half of the polarization is stable. An estimate of a possible compensation within the 10 ms can be obtained with the help of the Maxwell relaxation time, which shows, however, that only a fraction of about 10^{-4} of the total charges needed for a complete compensation
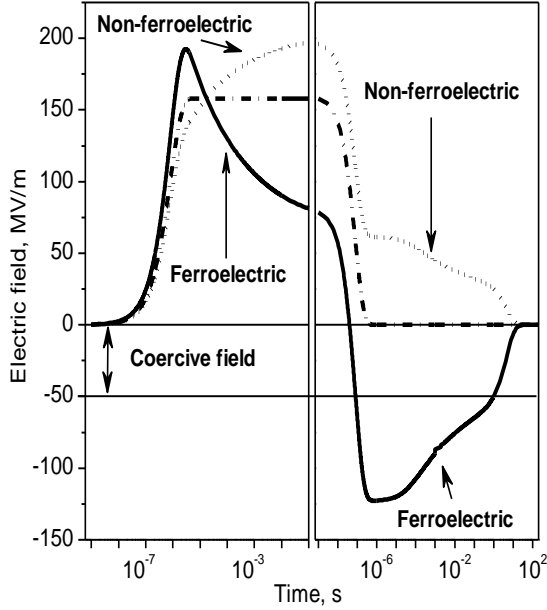
Fig. 8 – Calculated development of the field strength in the ferroelectric (solid line) and nonferroelectric (dotted line) components of PVDF during initial poling at 2 kV for 10 ms (left figure) and subsequent short circuiting (right figure). The average field is shown by a dash-dotted line

were able to reach the crystallites. Therefore conductivity cannot be accounted responsible for stabilization of the remaining polarization since no sizable amount of charge was delivered to the polarized crystallites or dipoles as was claimed by the Eisenmenger model to be necessary for the stability of the polarization [12].

Despite some deviations, the overall comparison of experimental and calculated dynamics of the ferroelectric polarization during initial poling and short circuiting shows not only qualitative but also quantitative agreement between the two, indicating that the model suggested for initial poling of a two-component ferroelectric [22, 24] is valid also for the explanation of the back switching phenomenon. The back-switched polarization is very small or zero at small and very long poling times and reaches a maximum at intermediate poling times.

5. SWITCHING OF POLARIZATION

To analyze the switching of polarization, the same model has been used as for initial poling and short-circuiting. Initial conditions are as follows: $P_F(0) = P_0$, $E_1(0) = E_2(0) = 0$. However, the case of polarization switching compared to initial poling and short circuiting is more complex, because the behavior of the already trapped charges is not clear. It is obvious that the trapped charges will be released and then retrapped. This means that the conductivity induced by the respective density of the freed charges has to be superposed on the intrinsic conductivity assumed above. This means the number of free charge carriers will be changed during polarization switching affecting the dynamics of the ferroelectric polarization.

In order to reveal the effect of screening and conductivity on the switching process, four extreme cases of the screening charge behavior during switching of polarization were considered:

Case 1: Gradual release of screening charges during switching from $P_F(0) = -P_0$ to $P_F(\infty) = +P_0$ followed by re-establishing of screening. Recombination of released charges is considered;

Case 2: Instant release of the screening charge at the moment of switching voltage application accompanied by recombination and re-establishing of screening;

Case 3: High intrinsic conductivity during the polarization switching;

Case 4: Low intrinsic conductivity with release of the screening charge by means of Maxwell relaxation time.

In the following, the current equation (1) is used for all four cases. The conductivity is now assumed to be $g = g_0$ for case 4 and $g = g_0 + en_f\mu$ for cases 1, 2 and 3 with e being the elementary charge, μ the mobility of the free charge carriers and n_f the free charge density.

Considering gradual release and recombination in case 1, the dynamics of the charge density n_f is formulated as follows

$$\frac{dn_f}{dt} = 2n_f \frac{dP/dt}{ed} - \alpha n_f^2 \qquad (15)$$

where the first term on the right side describes the released charge density due to polarization switching and the second term shows the charge recombination.

For case 2 all screening charges are released instantaneously described by

$$\frac{dn_f}{dt} = -\alpha n_f^2 \qquad (16)$$

with the initial condition

$$n_f(0) = n_0 = \frac{2n|P_0|}{ed} . \qquad (17)$$

In case 3 of high intrinsic conductivity, g is the same as the initial value in case 2

$$g = g_0 + \frac{2n|P_0|}{ed}\mu , \qquad (18)$$

whereas $g = g_0$ is assumed in case 4 of low conductivity.

The intrinsic polarization dynamics in all four cases is described by equations (1) and (15). The hysteresis of the ferroelectric polarization is simplified by

$$P_F(E_2) = \begin{cases} -P_o & E_2 \leq E_c \\ -P_o + 2P_o \dfrac{E_2 - E_c}{E_{sat} - E_c}; & E_c \leq E_2 \leq E_{sat} \\ +P_o & E_2 > E_{sat} \end{cases} . \quad (19)$$

Equations (1) and (15) to (19) were solved numerically and the corresponding results for the ferroelectric polarization P are presented in Figure 9.

The best fitting was obtained for case 2 with the following values of parameters: $\mu = 10^{-11}$ m²/V s, $\tau_0 = 2 \cdot 10^{-8}$ s, $E_A = 1.1 \cdot 10^9$ V/m, and $a = 0.5 \cdot 10^{-20}$ m³/s. The same parameters were used in calculations of case 1. In case 3, $n_f = n_0 = 3.92 \cdot 10^{26}$ m⁻³ causing $g = g_{max} = 6.32 \cdot 10^{-4}$ S/m, while $n_f = 0$ and $g = g_0 = 3 \cdot 10^{-11}$ S/m corresponded to case 4. In all models it is assumed that the initial polarization before switching is completely screened by charges at the ferroelectric boundaries.
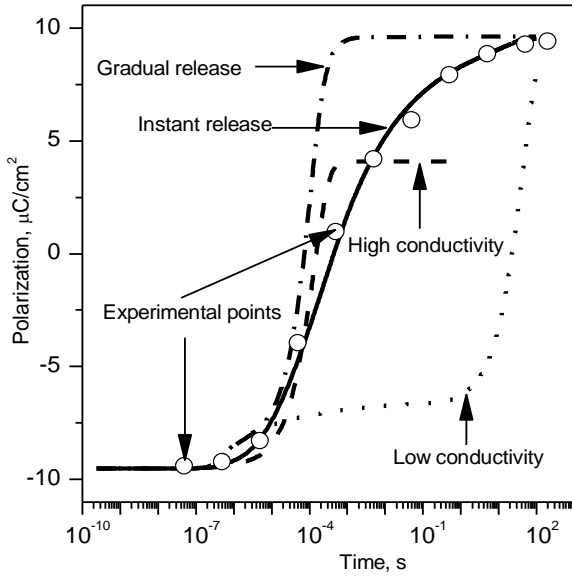
Fig. 9 – Polarization switching dynamics under condition of gradual release of the screening charges, instant release, high conductivity and low conductivity compared to experimental data shown by square points

The charges are presumably not deeply trapped but electrostatically weakly fixed to the bound surface charges of the ferroelectric layers. The isotropic conductivity, assumed everywhere in the sample, guaranties that charges can flow throughout the whole sample and mask the structural difference between the existing ferroelectric nanoparticles in an amorphous matrix and the layered system in the present theoretical model.

It is clear from Figure 9 that the best agreement between experimental and theoretical dynamics of the polarization switching is observed in case 2 corresponding to an instantaneous release of the screening charges upon application of the switching voltage. With all other models, a fit of the theoretical prediction to the experimental data was unsuccessful, as can be seen from Fig. 9.

The physical reason why all other models fail can be seen in the dynamics of the released charges. In the model with constant low conductivity (case 4) the charges are released according to the Maxwell relaxation time constant $\tau_M = \varepsilon_0 \varepsilon / g_0$, which is $\tau_M = 4.5$ s in the present case. The consequence is that only a small fraction of the polarization can switch freely, whereas the rest is hindered by the electric field of the still persisting screening charges. This situation changes around the Maxwell relaxation time when the screening charges are released. Too fast increase is observed for the high conductivity case 3 where $\tau_M = 4.2 \cdot 10^{-7}$ s. In this case the screening charges are released almost instantaneously. The reversed polarization increases faster than the experiment until the high conductivity limits the voltage increase due to a voltage division between the sample resistance of about 2000 Ω and the external resistance of $R = 500$ Ω.

In the case 1 of gradual release, the polarization behaves like a transition from low to high conductivity. Initially the conductivity is too low leading to signs of polarization saturation and later it is too high resulting in a too
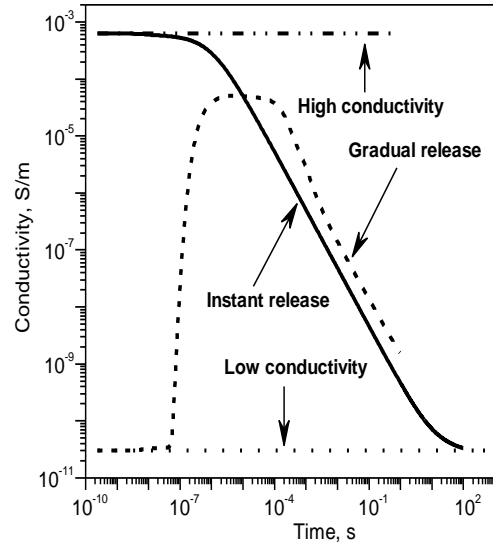

Fig. 10 – Calculated dynamics of the conductivity during the polarization switching under condition of gradual release of the screening charges, instant release, high conductivity and low conductivity
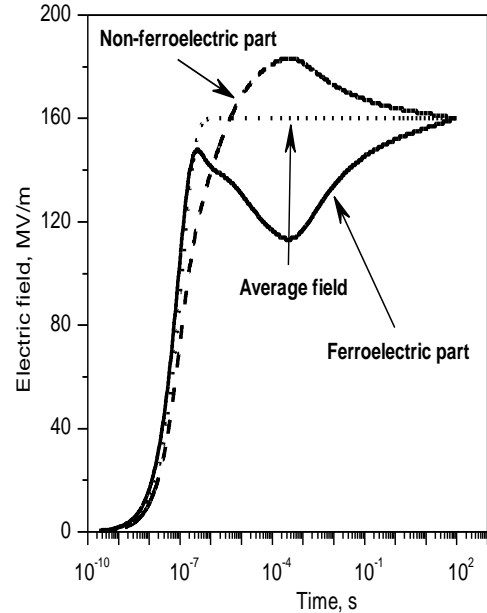

Fig. 11 – Calculated dynamics of fields in nonferroelectric and ferroelectric parts of the sample during the polarization switching in the case 2 of instant release of the screening charges

fast build-up of the polarization. The respective temporal development of the conductivity is shown in Figure 10.

The model of instantaneous release (case 2) seems to offer the right mix of released charge, recombining charge and conducting charge. The initially very high number of released charges forms a high conductivity that allows polarization to switch unimpeded. The reduced switching rate compared to the low conductivity case 4 can be seen in the reduced switching voltage due to the above mentioned voltage division. Since the recombination is controlled by equation (17), a very fast reduction of the conductivity occurs, as can be seen in Figure 10, resulting in an impeded increase of polarization (see Figure 9). One way of looking at it would be a

gradual changing Maxwell's relaxation time from $\tau_M = 4.2 \cdot 10^{-7}$ s to $\tau_M = 4.5$ s.

Figure 11 displays the dynamics of the electric field evolution in the closest to experiment case 2, which exhibits the complicated interplay between the external electric field, the polarization and the screening charge in the non-ferroelectric and ferroelectric regions. One notices that the electric field in the ferroelectric part drops below the average field due to build-up of polarization and lack of sufficient screening.

6. CONCLUSION

By comparing the experimental dynamics of the ferroelectric polarization in PVDF during initial poling, short circuiting and polarization switching with the theoretical one obtained from the two-layer model it is shown that the conductivity and space charge play an important role in obtaining the high and stable ferroelectric polarization. The conductivity during initial poling is responsible for the second slow part of the polarization build-up. In the case of short circuiting after initial poling, the conductivity prevents undesired back-switching of the formed polarization. During the switching of polarization, the critical dependence of the polarization phenomena on conductivity was also revealed. The authors strongly believe that the discovered features related to effect of conductivity, in general, are characteristic not only for ferroelectric polymers, but also for other two-component ferroelectric systems, such as the ferroelectric ceramics and polymer-ferroelectric composites.

ACKNOWLEDGMENT

REFERENCES

1. *Electrets,* **1**, (3rd edition, Ed. G.M. Sessler) (Morgan Hill: Laplacian Press: 1999).
2. H. Kawai, *Jpn. J. Appl. Phys.* **8**, 975 (1969).
3. J.G. Bergman, J.H. McFee, G.R. Crane, *Appl. Phys. Lett.* **18**, 203 (1971).
4. T. Furukawa, M. Date, E. Fukada, Y. Tajitsu, A. Chiba, *Jpn. J. Appl. Phys.* **19**, L109 (1980).
5. A.J. Lovinger, *Development in Crystalline Polymers*, (Ed. D.C. Bassett), (London and New Jersey: Applied Science Publications: 1982).
6. R. Gerhard-Multhaupt, *Ferroelectrics* **75**, 385 (1987).
7. T. Furukawa, *Phase Transition* **18**, 143 (1989).
8. T. Furukawa, *Key Engineering Materials*, (Ed. D. K. Das-Gupta), (Switzerland: Trans. Tech. Publications: 15 1994).
9. R.G. Kepler, R.A. Anderson, *Adv. Phys.* **41**, 1 (1992).
10. G.M. Sessler, *Key Engineering Materials*, (Ed. D.K. Das-Gupta), (Switzerland: Trans. Tech. Publications: 249 1994).
11. R.G. Kepler, *Ferroelectric Polymers*, (Ed. H.S. Nalwa), (New York: Marcel Dekker: 183 1995).
12. G. Eberle, H. Schmidt, W. Eisenmenger, *IEEE T. Dielectr. Electr. Insul.* **3**, 624 (1996).
13. M.G. Broadhurst, G.T. Davies, *Ferroelectrics* **32**, 177 (1981).
14. T. Furukawa, G.E. Johnson, *Appl. Phys. Lett.,* **38**, 1027 (1981).
15. R. Hayakawa, Y. Wada, *Adv. Polym. Sci.* **11**, 1 (1973).
16. N. Murayama, *J. Polym. Sci.: Polym. Phys.* **13**, 929 (1975).
17. Y. Wada, R. Hayakawa, *Jpn. J. Appl. Phys.* **15**, 2041 (1976).
18. M.G. Broadhurst, G.T. Davis, J.E. McKinney, R.E. Collins, *J. Appl. Phys.* **49**, 4992 (1978).
19. P.D. Southgate, *Appl. Phys. Lett.* **28**, 250 (1976).
20. G.T. Davis, M.G. Broadhurst, A.J. Lovinger, T. Furukawa, *Ferroelectrics* **57**, 73 (1984).
21. H. von Seggern, S. Fedosov, *IEEE T. Dielectr. Electr. Insul.* **7**, 543 (2000).
22. H. von Seggern, S.N. Fedosov, *Appl. Phys. Lett.* **81**, 2830 (2002).
23. S.N. Fedosov, H. von Seggern, *J. Appl. Phys.* **96**, 2173 (2004).
24. H. von Seggern, S. Fedosov, *IEEE T. Dielectr. Electr. Insul.* **11**, 232 (2004).
25. H. von Seggern, S.N. Fedosov, *Appl. Phys. Lett.* **91**, 062914 (2007).
26. S.N. Fedosov, H. von Seggern, *J. Appl. Phys.* **103**, 014105 (2008).
27. W. Eisenmenger, M. Haardt, *Solid State Commun.* **41**, 917 (1982).
28. M. Womes, E. Bihler, W. Eisenmenger, *IEEE T. Electr. Insul.* **24**, 461 (1989).
29. G.M. Sessler, D.K. Das-Gupta, A.S. DeReggi, W. Eisenmenger, T. Furukawa, J.A. Giacometti, R. Gerhard-Multhaupt, *IEEE T. Elec. Insul.* **27**, 872 (1992).
30. T. Furukawa, K. Suzuki, M. Date, *Ferroelectrics* **68**, 33 (1986).
31. M.E. Lines, A.M. Glass, *Principles and Applications of Ferroelectrics and Related Materials,* (Oxford: Oxford University Press: 2001).
32. J.C. Burfoot, C.W. Taylor, *Polar Dielectrics and Their Application*, London: Macmillan: (1979).
33. E.L.V. Lewis, I.M. Ward, *J. Polym. Sci. Part B: Polym. Phys.* **27**, 1375 (1989).
34. V.I. Arkhipov, S.N. Fedosov, D.V. Chramchenkov, A.I. Rudenko, *J. Electrostat.* **22**, 177 (1989).
35. G.F. Leal Ferreira, R.A. Moreno, *Ferroelectrics* **189**, 63 (1996).